Available online at www.sciencedirect.com

ScienceDirect

journal homepage: www.intl.elsevierhealth.com/journals/dema

Biomimetic transformation of polyphosphate microparticles during restoration of damaged teeth

Maximilian Ackermann[a], *Emad Tolba*[b,c], *Meik Neufurth*[b], *Shunfeng Wang*[b], *Heinz C. Schröder*[b], *Xiaohong Wang*[b], *Werner E.G. Müller*[b,*]

[a] *Institute of Functional and Clinical Anatomy, University Medical Center of the Johannes Gutenberg University, Johann Joachim Becher Weg 13, D-55099 Mainz, Germany*

[b] *ERC Advanced Investigator Grant Research Group at the Institute for Physiological Chemistry, University Medical Center of the Johannes Gutenberg University, Duesbergweg 6, D-55128 Mainz, Germany*

[c] *Polymers and Pigments Department, National Research Center, 33 El Buhouth St, Dokki, 12311 Cairo, Egypt*

ARTICLE INFO

Article history:
Received 29 July 2018
Received in revised form
1 November 2018
Accepted 14 November 2018

Keywords:
Inorganic polyphosphate
Microparticles
Dentifrice
Alkaline phosphatase
Coavervate
Regeneration
Enamel/dentin damage repair
Caries

ABSTRACT

Objective. In the present study, we investigated the fusion process between amorphous microparticles of the calcium salt of the physiological polymer comprising orthophosphate units, of inorganic polyphosphate (polyP), and enamel.

Methods. This polymer was incorporated as an ingredient into toothpaste and the fusion process was studied by electron microscopy and by synchrotron-based X-ray tomography microscopy (SRXTM) techniques.

Results. The data showed that toothpaste, supplemented with the amorphous Ca-polyP microparticles (aCa-polyP-MP), not only reseals tooth defects on enamel, like carious lesions, and dentin, including exposed dentinal tubules, but also has the potential to induce re-mineralization in the enamel and dentin regions. The formation of a regeneration mineralic zone on the tooth surface induced by aCa-polyP-MP was enhanced upon exposure to artificial saliva, as demonstrated by SRXTM. Energy dispersive X-ray analysis revealed an increase in the calcium/phosphorus atomic ratio of the enamel deposits to values characteristic for the particles during the treatment with polyP applied in the toothpaste, indicating a fusion of the particles with the tooth mineral.

Significance. Our results suggest that toothpaste enriched with aCa-polyP-MP is a promising biomimetic material for accelerating enamel and dentin restoration.

1. Introduction

Dental restoration/dental filling aims to treat and to restore the function, integrity, and morphology of missing tooth structure occurring as a consequence of caries or of external trauma. Such a closing of space, where bacteria could enter, also helps to prevent further decay. At present the materials used for fillings include gold, porcelains, defined composite resins and amalgams. Those components are regeneratively inert, since they are not included in a repair or a remodeling process of the decayed tooth, or of the surrounding tissue (reviewed in Ref.: [1]). However, there are nanotechnology-

* *Corresponding author.*
E-mail address: wmueller@uni-mainz.de (W.E.G. Müller).

https://doi.org/10.1016/j.dental.2018.11.014

based restorative materials that are currently intensively developed [2], as well as regeneratively active biomaterials [3] that are advanced rapidly in the field of repair of bone and bone-derived rigid organs. These developments are driven by new spectacular discoveries in the field of biomaterial sciences.

Minerals are ubiquitous components of living systems from bacteria to plants and the different animal phyla where they accomplish an array of crucial structural and functional roles. While minerals in the non-living world are usually formed at extreme temperatures and pressures and over long geological timespans, biogenic minerals are synthesized at physiological, ambient temperatures and pressures, eventually leading to crystal formation. For these biological processes, the term biomineralization has been coined [4,5]. In 1988 [6], it has been postulated that proteinaceous templates control crystal growth *via* their functional groups through precise stereochemical coordination of metal atoms. Other organic templates, like complex carbohydrates, have also been identified [7]. Since (almost) any kind of process in living organisms is enzymatically controlled, it was a matter of time to disclose these biocatalysts as causative factors involved in biomineralization.

The first enzyme found to be involved in biomineralization was silicatein, a cathepsin-related enzyme that forms the basis for the synthesis of biosilica in sponges ([8,9]; reviewed in Refs.: [10,11]). In addition, it has been demonstrated that silicatein comprises not only an enzymatic activity but also a structure-guiding function during the mineralization process [12,13]. More recently, the first enzymes involved in the formation of bone and dentin mineral, carbonated apatite/hydroxyapatite, have been identified. Since hydroxyapatite [HA] contains a considerable amount of carbonate besides of 50% octacalcium phosphate (47% carbonate apatite with about 2% calcium carbonate), especially during embryogenesis [14], the enzyme carbonic anhydrase has been proposed to be the initiating enzyme during bone formation [15]. Considering the basic premise that crystalline biomaterials are formed *in vivo* from amorphous precursors [16], it is proposed that the amorphous calcium carbonate [ACC] in the bone mineral is a product of the carbonic anhydrase reaction [17], a view also shared by Weiner et al. [16]. ACC is converted into the calcium phosphate mineral, again in the amorphous phase [17], a process that is driven non-enzymatically and exclusively thermodynamically. The product formed is amorphous calcium phosphate [ACP], from which the crystalline HA maturates [18].

ß-Glycerophosphate has been shown to be a potent phosphate donor *in vitro* [19]. However, *in vivo* this metabolite is unlikely to be an efficient source for phosphate as it is rapidly hydrolyzed by extracellular alkaline phosphatase [ALP] [20]. Another phosphate source for bone mineralization is polyphosphate [polyP] [21], an abundant inorganic polymer found in human/animal body fluids as well as intracellularly, particularly in the megakaryocyte-derived cell fragments, the blood platelets [22]. Physiologically, this polymer consists of about 40–100 phosphate units which are linked by high-energy phosphoanhydride bonds. The main polyP-degrading enzyme is the ALP [23,24]. Recent studies have shown that enzymatic cleavage of polyP by ALP transfers metabolic energy to ADP, from which phosphorylation to ATP is likely to occur *via* the adenylate kinase [25,26]. The encapsulation of polyP as amorphous particles [27], as in the acidocalcisome [28], opens a new avenue for the application of polyP as a smart regeneratively active biomaterial for tissue engineering [29].

ACP [$Ca_3(HPO_4)_{3\nu}(PO_4)_{3y}\cdot zH_2O$], the putative precursor for bone HA readily occurs in aqueous solution by precipitation through multiple intermediates, often with a further ACP-stage and an octacalcium phosphate phase [$Ca_8H_2(PO_4)_6\cdot 5H_2O$] until the formation of the crystalline calcium phosphate (reviewed in Ref.: [30]). *In vitro*, the solid phase ACP precipitates from a highly supersaturated phosphate solution and is then readily converted to octacalcium phosphate or apatite ($Ca_{10\text{-}x}(HPO_4)_x(PO_4)_{6\text{-}y}(OH)_{2\text{-}x}$). Applying a variety of techniques, including cryo-TEM, *in situ* as well as *ex situ* procedures, ACP has been shown to crystallize forming nanometre-sized units of calcium triphosphate complexes. During this apatite formation process, the precursors take up an additional Ca^{2+} ion and form fractal clusters of $Ca_2(HPO_4)_3^{2-}$. From this stage, the crystal structure of octacalcium and apatite maturates [31]. Unlike the chemically synthesized apatite (geological apatite), bone HA is formed around a collagen scaffold [32] and does not have a hexagonal crystal morphology; it is described as a monoclinic apatite [33,34]. Moreover, the bone HA is only poorly crystalline due to the small size of the crystals, the residual stresses in the crystal lattice, and ionic substitutions, such as of PO_4^{3-} by HPO_4^{2-}, or of Ca^{2+} by Na^+, Sr^{2+}, Mg^{2+}, or Zn^{2+} [35,36].

It has been proposed that inorganic pyrophosphate is a regulator of bone HA synthesis both under pathological and physiological conditions [37] and presumably inhibits the ALP [38]; a large amount of data has been gathered indicating that the enzyme promotes calcification by lowering pyrophosphate levels ([39]; reviewed in Ref.: [40]). This view is supported by the demonstration that cells present in calcifying cartilage and resorbing bone are rich in ALP [41]. Using the biomimetic approach but using polyP instead of pyrophosphate, we prepared stable ACP in the presence of <10 wt.% of the polymer [42]. So far, no data are available on the possible presence of polyP in the HA biomaterial *in vivo*. However, the accumulation of blood platelets at sites of bone damage or injury (reviewed in Ref.: [43]) and the observation that platelet-rich plasma accelerates the healing of musculoskeletal injuries (reviewed in Ref.: [44]) support the proposition that polyP released from the blood platelets contributes to HA formation. In the extracellular space, polyP is hydrolyzed by ALP [23]. The existence of this enzyme in the saliva is well known [45].

In previous studies, we reported that amorphous polyP, encapsulated into microparticles as an amorphous Ca^{2+} salt, aCa-polyP-MP, efficiently seals open dentinal tubules exposed at the tooth surface [46]. In subsequent analyses, we have formulated a toothpaste composition containing aCa-polyP-MP that efficiently reduced dental biofilm formation [47] and induced the remineralization process [48]. In the present study, we apply the technique of synchrotron-based X-ray tomographic microscopy (SRXTM) [49,50] to demonstrate the fusion process between the microparticles and the tooth enamel. It is found that the enamel becomes covered by an induced mineralization material when the polyP-treated paste is submersed in an artificial saliva fluid. This induced miner-

alization process does not occur on non-treated enamel. The amalgamation of aCa-polyP-MP with the tooth mineral is also supported by energy dispersive X-ray analysis [EDX] which revealed that with increasing duration of the polyP treatment, applied in the dentifrice, the calcium/phosphorus atomic ratio increased from 0.72 ± 0.13 to 1.50 ± 0.23 (6 d treatment), a value close to that measured for human enamel (Ca/P atomic ratio, 1.43 ± 0.14).

2. Materials and methods

2.1. Materials

Sodium polyphosphate (Na-polyP) with an average chain length of ≈40 phosphate units was obtained from Chemische Fabrik Budenheim (Budenheim, Germany).

2.2. Preparation of polyP microparticles

aCa-polyP-MP, Ca^{2+}-polyP microparticles, were prepared from Na-polyP as described [27]. Na-polyP was dissolved in distilled water, then treated with a 2-fold weight ratio of $CaCl_2 \cdot 2H_2O$ (#223506; Sigma-Aldrich, Taufkirchen, Germany) at pH10 (room temperature) and stirred for 12 h. The microparticles formed were collected by filtration, washed with ethanol, and dried at 50 °C.

2.3. Composition of toothpaste

The complete procedure used for the preparation of the toothpaste has been given recently [47]. Diatomaceous earth was added as an abrasive and xylitol, xanthan, κ-carrageenan and glycerol were used as components of the dentifrice base. Where indicted, 3% [w/w] of aCa-polyP-MP (final concentration) was added.

2.4. Tooth samples

Human teeth (molar and premolar) were used as samples for the treatment with the experimental dentifrice. They were provided by the Institute of Functional and Clinical Anatomy, University Medical Center of the Johannes Gutenberg University, Mainz, Germany, following the ethical guidelines of the University Medical Center Mainz. The specimens were cleaned from organic material by incubation in 4% sodium hypochlorite solution for 4 h. Then the samples were thoroughly rinsed with distilled water and air dried.

2.5. Treatment of the teeth

The teeth samples were brushed with an electric toothbrush (Braun Oral-B PRO 6000; Procter & Gamble, Cincinnati; OH) at 8000 rpm and $100 \times g$ force for 3 min at room temperature [47]. An amount of ≈0.2 g of dentifrice was applied on top of the respective enamel and dentin surfaces. Routinely the specimens were brushed twice a day for 5 min each. Subsequently, the specimens were thoroughly rinsed. During the inter-brush periods, the teeth remained in a humid chamber.

2.6. Exposure to artificial saliva

The microparticles, aCa-polyP-MP, were applied as a glycerol suspension. The microparticles were suspended at a concentration of 3% [w/w] in 86% (v/v) aqueous glycerol, containing 2.5% xanthan gum (*Xanthomonas campestris*; #G1253 Sigma). This suspension was homogenized in a mortar and pestle to obtain a uniform mixing. From this 0.2 g were applied per tooth specimen for 2 d, and brushed twice daily. Then the specimens were transferred into the artificial saliva. In the control series, the specimens were treated with the plain glycerol suspension only.

The composition of the artificial saliva was chosen from the literature [51,52]. It contained 1 mM $CaCl_2$, 0.2 mM $MgCl_2$, 4.0 mM KH_2PO_4, 30.0 mM KCl, and 20.0 mM HEPES [(4-(2-hydroxyethyl)-1-piperazineethanesulfonic acid]). The pH was adjusted to 7.0 (KOH). The tooth samples were submersed in an excess of solution.

2.7. Microscopy

2.7.1. Digital light microscopy

The analyses were performed with a VHX-600 Digital Microscope (Keyence, Neu-Isenburg; Germany), equipped with a VH-Z100 zoom lens.

2.7.2. Electron microscopy

For high-resolution scanning electron microscopic (SEM) analysis, a HITACHI SU 8000 (Hitachi High-Technologies Europe GmbH, Krefeld, Germany) equipped with a low voltage (<1 kV) near-surface organic surfaces detector was used. The samples were processed without further sputtering. Lower-resolution inspections were made with an ESEMXL-30 machine (Philips, Eindhoven; The Netherlands). The teeth were dehydrated in ethanol, freeze-dried, mounted onto specimen holders and finally sputtered with gold in an argon atmosphere as described.

2.8. Synchrotron-based X-ray tomographic microscopy

The non-destructive high-resolution technique of synchrotron-based X-ray tomographic microscopy (SRXTM) was used as described before [49,50]. Imaging recording was performed at the TOMCAT-beamline of the Swiss Light Source at the Paul Scherrer Institute (Villigen; Switzerland).

2.9. Energy dispersive X-ray spectroscopy

For the experiments, an EDAX Genesis EDX System attached to a scanning electron microscope (Nova 600 Nanolab, FEI, Eindhoven; The Netherlands) and operating at 10 kV with a collection time of 30–45 s was applied. The system was calibrated with standard samples, allowing measurements with an error of approximately 10% [53].

2.10. Statistical analysis

The results were statistically evaluated using the paired Student's *t*-test [54].

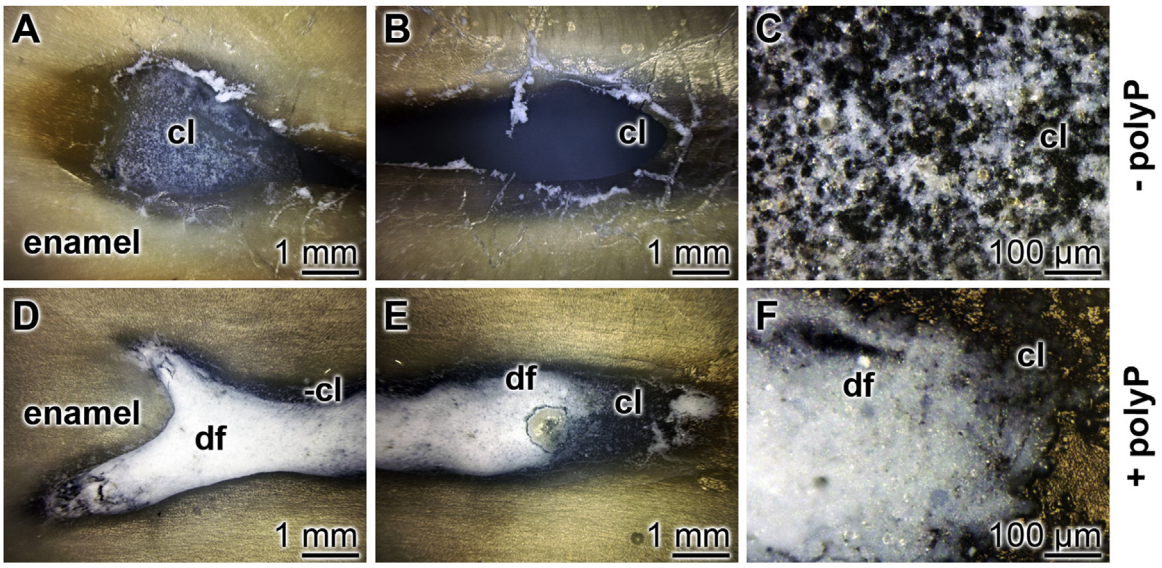

Fig. 1 – Brushing of the enamel surface of human teeth with the toothpaste without polyP (A–C), or with the paste supplemented with 3% [wt/wt] of aCa-polyP-MP (D–F). Onto the surface areas of teeth brushed with the aCa-polyP-MP-containing toothpaste, extensive areas remained covered with dentifrice (df) onto the carious, decayed regions (cl). The paste was applied for a period of 6 d.

3. Results

3.1. *Sealing activity of the polyP-toothpaste: enamel*

The fabricated toothpaste containing 3% [w/w] of aCa-polyP-MP was applied to the enamel of the teeth and processed as described under Section 2. In parallel, the dentifrice without polyP was used as a control. After a 6 days' application/brushing (twice daily) on the tooth surfaces and after thorough rinsing the specimens with PBS [phosphate buffered saline], no extensive plaques on the decayed carious teeth that might have originated from the paste adhered to the enamel in the series with dentifrice without polyP (Fig. 1A–C). In contrast, large areas of dentifrice remained on comparable surfaces of teeth treated with the aCa-polyP-MP-containing toothpaste (Fig. 1D–F) when analyzed with light microscopy.

Closer inspection of the enamel surfaces by SEM revealed that in the tooth series treated with dentifrice without polyP the vast majority of the cracks remained unsealed and had the appearance of cracks not treated at all (Fig. 2A). In contrast, most of the cracks within the enamel at the beginning of the treatment were sealed with tightly fitting material after the 6 days' brushing period (Fig. 2B). At high-resolution SEM inspection of the carious areas, plain highly-oriented HA crystals that are not covered by additional material are visible in the control samples (Fig. 2C). Fully developed mature dental enamel is seen, which comprises highly organized structures of enamel prisms consisting of bundles of nanorod-like HA crystals. The ribbon-like crystals measure 60–70 nm in width and 20–30 nm in thickness [55]. In contrast, the HA crystals in the carious lesions in the enamel of teeth samples brushed with the aCa-polyP-MP-containing toothpaste are covered with a layer of amorphous material (Fig. 2D). This material was identified by EDX as Ca-polyP (data not shown).

3.2. *Increase of the Ca/P atomic ratio of the dentifrice deposits with the duration of the application*

The Ca/P atomic ratio within the Ca-polyP microparticles has been previously determined to be 0.62 [26,27]. The deposits on the enamel of the aCa-polyP-MP-dentifrice after a one-day application measured a Ca/P atomic ratio of 0.72 ± 0.13 (number of independent measurements: 6); a representative EDX spectrum is given in Fig. 3A. This ratio increased significantly to 0.93 ± 0.18 ($p < 0.05$) after a 3 days' treatment (Fig. 3B) and even further to 1.50 ± 0.23 ($p < 0.01$) after a 6 days' application (Fig. 3C). This value is consistent with those published for pig enamel (1.52; [56]) and human enamel 1.92 [57]. In our approach, using the EDX (semi-)quantitative technique, we measured a value of 1.43 ± 0.14 for human enamel, a figure which matches the published data obtained by using the same analysis technique [58]. In contrast, when the scarcely occurring deposits from the polyP-lacking dentifrice were measured after 6 d, a Ca/P atomic ratio of 0.78 ± 0.17 was recorded.

3.3. *Sealing of the carious lesions/dentinal tubules with Ca-polyP-containing dentifrice*

Carious lesions appear in the enamel and may gradually spread to the dentin [59], exposing the HA crystals; Fig. 4A,B. In the deeper regions, the dentinal tubules are seen that extend from the dentino-enamel junction, or the dentino-cemental junction in the root area, to the outer wall. These tubules follow a radial or S-shaped path (Fig. 4C). In a comparative study, these carious lesions were treated either with the polyP-free control dentifrice (Fig. 4A,C,E) or the aCa-polyP-

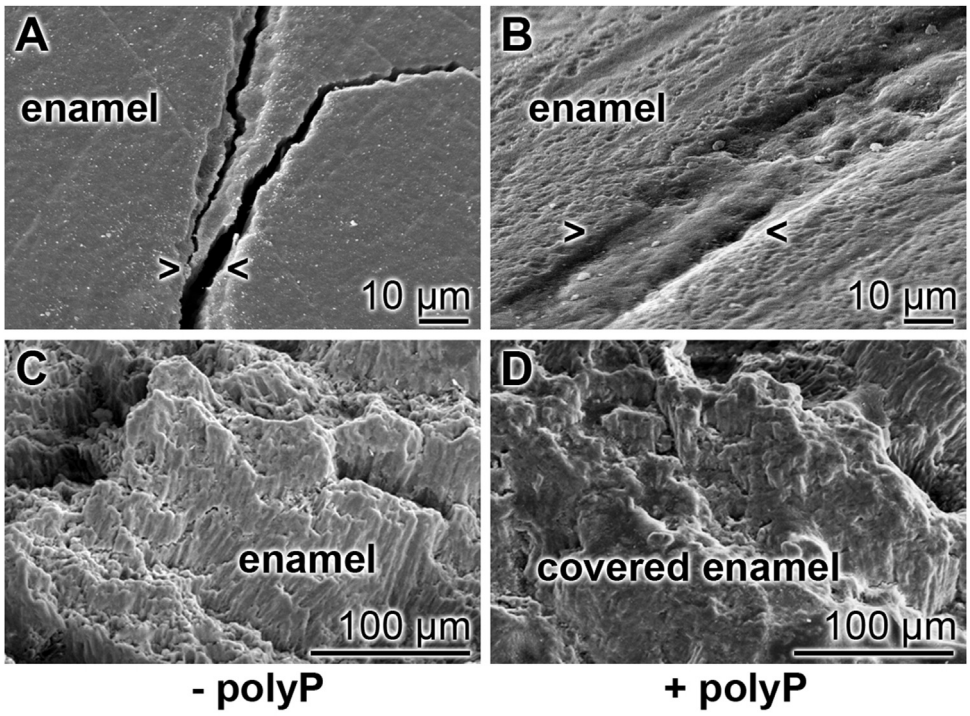

Fig. 2 – Sealing of carious areas on the enamel; high-resolution SEM. Tooth samples were treated with control dentifrice lacking polyP (A and C), or with dentifrice supplemented with 3% aCa-polyP-MP (B and D). In the samples treated with control toothpaste the cracks remained non-modified (> <) (A) and the mineral shows the characteristic, highly-oriented HA crystals (C). In contrast, in the test series with the aCa-polyP-MP-containing dentifrice the cracks are sealed (> <) (B) and the mineralic material is covered and does not expose the nanorod-like HA crystals (D).

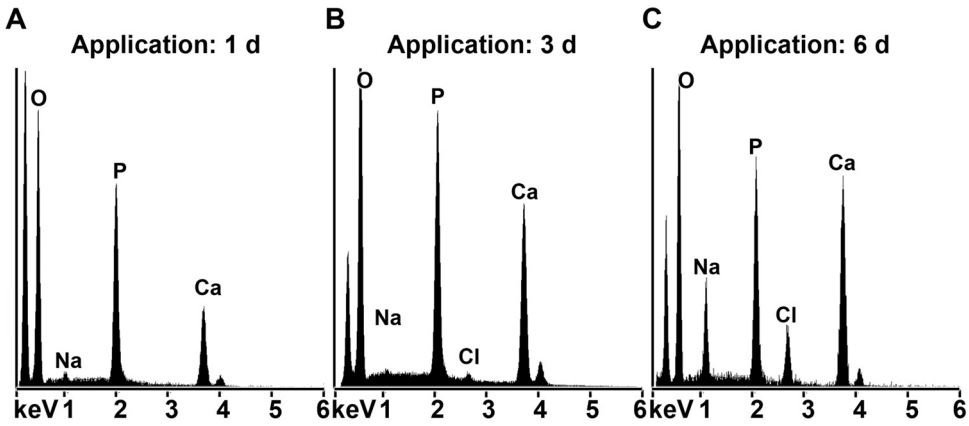

Fig.3 – Increase of the Ca/P atomic ratio in the deposits, formed after treatment with aCa-polyP-MP-containing dentifrice on enamel for 1 d (A), 3 d (B) and 6 d (C). The prominent peaks, including those for *Ca* and P are marked.

MP-supplemented dentifrice (Fig. 4B,D,F). Already after a 1 d application with the polyP-containing dentifrice, a relatively homogenous layer can be seen in the deeper regions of the lesions (Fig. 4B), which increases in continuity after 3 d and 6 d (Fig. 4D and F). In comparison, residual dentifrice areas are only occasionally seen in the polyP-lacking paste (Fig. 4A,C, and E).

The tooth dentin is traversed/radiated outwards with microscopic channels, the dentinal tubules that originate from the pulp and reach the exterior enamel-cementum border. The size of these tubules measures between 2 and 3 µm in diameter, depending on the demineralization stage [60]. If the tooth dentin regions are treated for 5 d with the control paste, the openings of the dentinal tubules are clearly visible (Fig. 5-IA,C,E) and their margins are sharp-edged (Fig. 5-IE). However, if the teeth are treated with polyP-enriched dentifrice for the same period of time, most of the tubules are either partially or completely sealed (Fig. 5-IB,D, and F). To demonstrate that the tubule is indeed sealed by polyP, an EDX scan was run

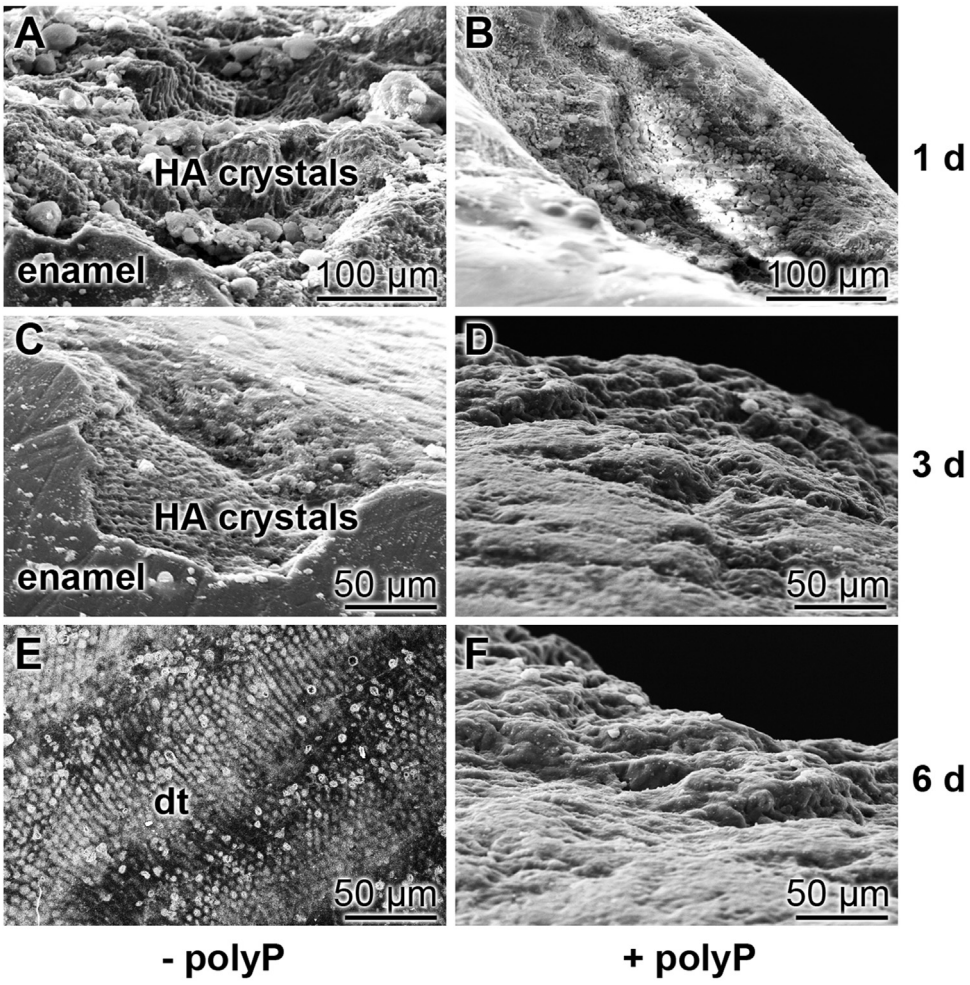

Fig. 4 – Protection of carious lesions on human teeth after treatment with polyP-lacking (A, C, E) and polyP-containing dentifrice (B, D, F). The pastes were applied for 1 d, 3 d, or 6 d, as indicated. In the series with polyP-lacking dentifrice, the morphology of the teeth could be delimited, while in the series with the aCa-polyP-MP-containing paste the developed layer covered the lesions. In E, the openings of the dentinal tubules (dt) are visible.

over the occlusion (Fig. 5II). The scan shows distinct peaks corresponding to Ca and P.

3.4. *Mineralization induction effects of polyP onto enamel surface*

It is known that artificial saliva can induce mineralization on the enamel surface [61]. For the study reported here, the artificial saliva was supplemented with 1 mM $CaCl_2$ and 4.0 mM KH_2PO_4 as described under Section 2.

To determine if polyP could cause any effect on the artificial mineralization process, the enamel surface remained either untreated (Fig. 6A and D) or was pretreated with polyP, applied as aCa-polyP-MP (Fig. 6B,C,E, and F). The microparticles were suspended in glycerol and then applied for 2 d onto the enamel. Already at this stage an almost homogeneous layer can be discerned (Fig. 6B); at higher magnification, the individual microparticles can be visualized (Fig. 6C and F). If the samples, non-treated or polyP-treated, are immersed in artificial saliva and incubated there for 5 d, a striking difference in the mineralization pattern is seen. While in the non-pretreated control samples, the mineralic deposits are individually layered onto the top of the enamel (Fig. 6D), continuous layers of deposits are formed on the enamel pretreated with polyP (Fig. 6E).

Synchrotron-based tomographic imaging was applied to study the crystal organization on the border between the enamel and the mineral deposits formed during the incubation with the artificial saliva (Fig. 7). In the controls not treated with polyP, only the genuine enamel layer is visible (Fig. 7A). However, onto the enamel samples brushed with aCa-polyP-MP glycerol, an additional layer composed of "induced material", as termed here, appeared (Fig. 7B–D). Furthermore, bulky deposits originating from the artificial saliva can be distinguished. Interestingly, this material is not seen in the controls, underscoring the mineralization inducing property of polyP.

4. Discussion

Dental enamel is the hardest tissue in mammals and consists to ≈95% of carbonated hydroxyapatite. The inorganic deposits

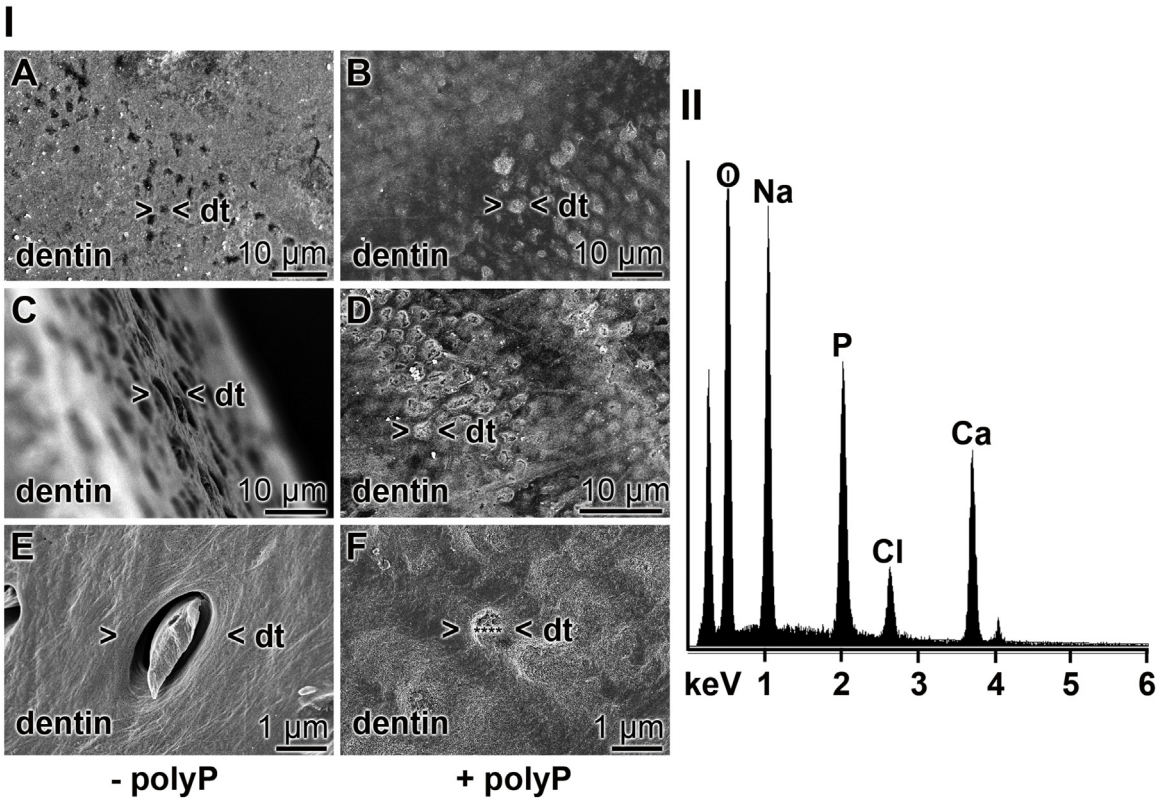

Fig.5 – Sealing of the openings of the dentinal tubules with polyP. (I) REM analysis. (A, C, E) The surfaces of the exposed dentinal tubules (dt) traversing the dentin region to the enamel border are treated for 5 d with polyP-free dentifrice. The dentin surface and the openings of the dentinal tubules are clearly visible. (B, D, F) Treatment of those surfaces for the same period of time (5 d) with the aCa-polyP-MP-containing dentifrice results in a sealing of the openings. (II) EDX analysis. The spectroscopic scan was performed over one sealed dentinal tubule (marked in F, **).**

are formed during the biomineralization process onto matrix proteins (amelogenin, ameloblastin and enamelin) which are secreted by ameloblasts and serve as guidance. This matrix allows the formation of individual HA "rods" or "prisms" that grow appositionally away from the dentino-enamel junction [62]. Finally, most of the organic matrix is metabolized by proteases. The basic units of tooth enamel, the rods, measure ≈4 μm in width to ≈8 μm in height and consist of highly organized HA [63]. In the dentin, the crystals are about 50 nm in length, 20 nm in width and 2–5 nm in thickness [64]. As in bone, dentin collagen and its associated proteins play the dominant role in determining the mineralization process. The content of organic materials within the dentin is larger and amounts to ≈33% (by weight), while the content of HA is about 45%. Because of these factors, especially the low content of cells and organic matrices in the enamel, the enamel acid cannot re-calcify [65].

Until now, the controversy over the presence of an ACP has not been solved, since complex structural analyses have failed to detect the presence of ACP in young bone [66]. Nonetheless, the physiological HA differs from the geological form by the smaller crystal size, the high degree of carbonate substitution combined with a substantial OH deficiency, and the presence of lattice vacancies that render the bone and teeth HA more soluble (see Ref.: [67]). The smaller size of the physiological HA makes it more soluble, as more atoms are exposed on the surfaces of the HA crystals. This property allows the incorporation of carbonate substitutions that result in the transition of the poorly crystalline HA with high HPO_4^{2-} content to a biomineral of higher crystallinity, lower phosphate content, and a more complex crystal organization that still contains carbonate substitutions [68,69]. Taken together, the biomineralization of bone tissue, in contrast to the geological HA mineralization, can undergo a remodeling which is comparatively high in bone and dentin and very low in enamel. Especially in the latter material, HA is prone exclusively to physical dissolution processes by bacterial and environmental acids [70].

Critical for the durability of the mineralic matrix of teeth is the pH, which is at pH 5.5. Above this value, the mineral environment is supersaturated with the mineral, and the additional mineral tends to precipitate [71]. Conversely, the milieu is unsaturated at lower pH values in the surroundings, resulting in dissolution processes. As outlined in the Section 1, polyP is a promising inorganic and physiological polymer for potential use in restoration of HA in teeth [26,46,47]. In particular, when formulated in microparticles such as aCa-polyP-MP, release of the polymer from the biomimetically fabricated particles and subsequent hydrolytic cleavage by the ALP is slower than with soluble Na-polyP. The following properties of polyP qualify this polymer. As outlined in the Section 1, polyP is a readily available component for HA formation after enzymatic

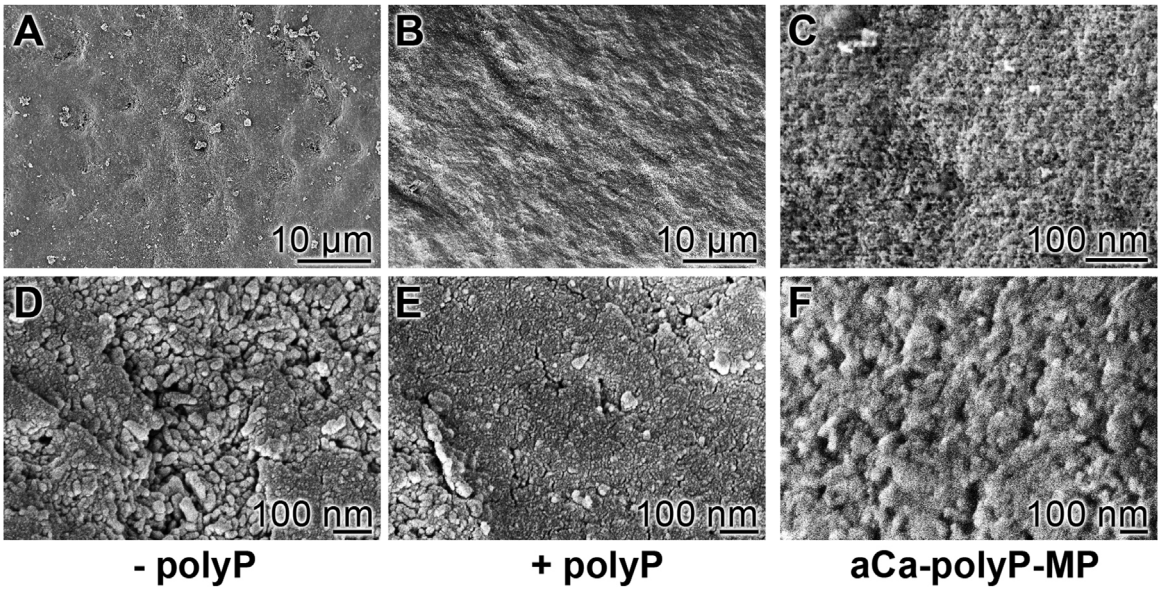

Fig. 6 – Homogeneous layer-formation on enamel after a pretreatment with polyP. The polymer was added as aCa-polyP-MP. The enamel remained either untreated (- polyP) (A and D) or was treated with polyP, as described under Section 2 (B, C, E and F). After 2 d of application the particles already coalesce onto the surface of the enamel (B). If the samples were further processed by submersing into artificial saliva, additional crystals formed onto non-pretreated enamel remain separate and craggy (D), while the deposits onto the polyP-pretreated specimens form a continuous layer (E). The two images C and F show the microparticles on the enamel after the 2 d application.

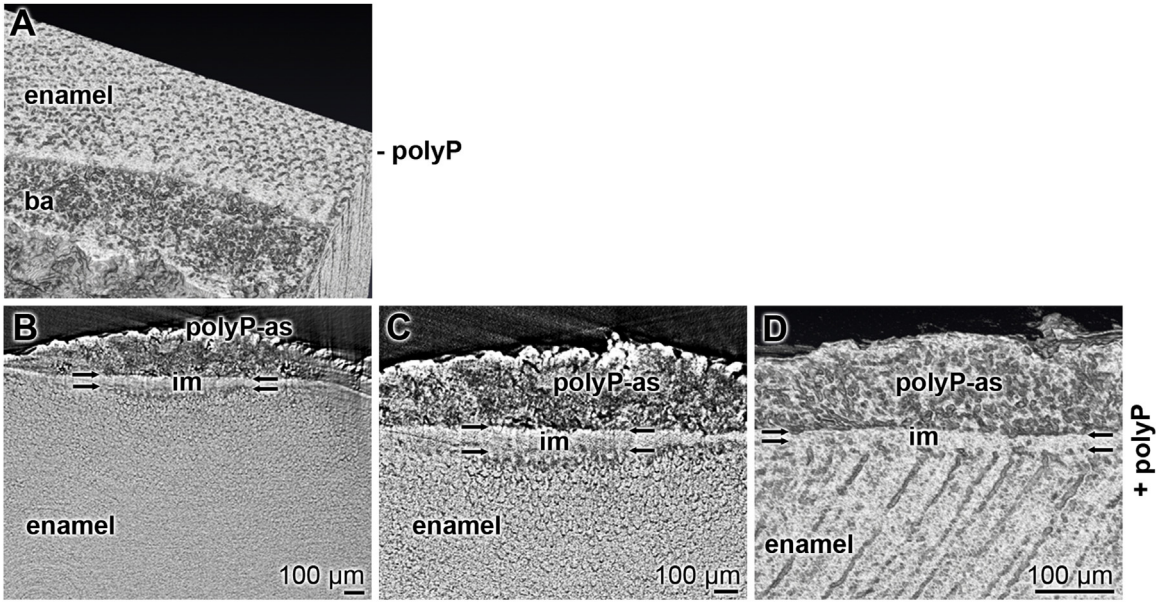

Fig. 7 – Induced mineralization on enamel specimens. The teeth samples were treated either with the plain glycerol solution only (A), or with the aCa-polyP-MP-containing glycerol solution (B–D) for 2 d, and then transferred to artificial saliva. After incubation for 5 d the specimens were inspected by synchrotron-based X-ray tomographic microscopy. In the control sample (A) the enamel surface is distinctly to discern in addition to the brushing area (ba). No additional layer is seen. In contrast, in the polyP-treated samples (B–D), the enamel zone is clearly and additionally over-layed by an induced material (im) which is most likely attributable to polyP. The specimens are surrounded by deposits which are contributed by the polyP-artificial saliva (polyP-as).

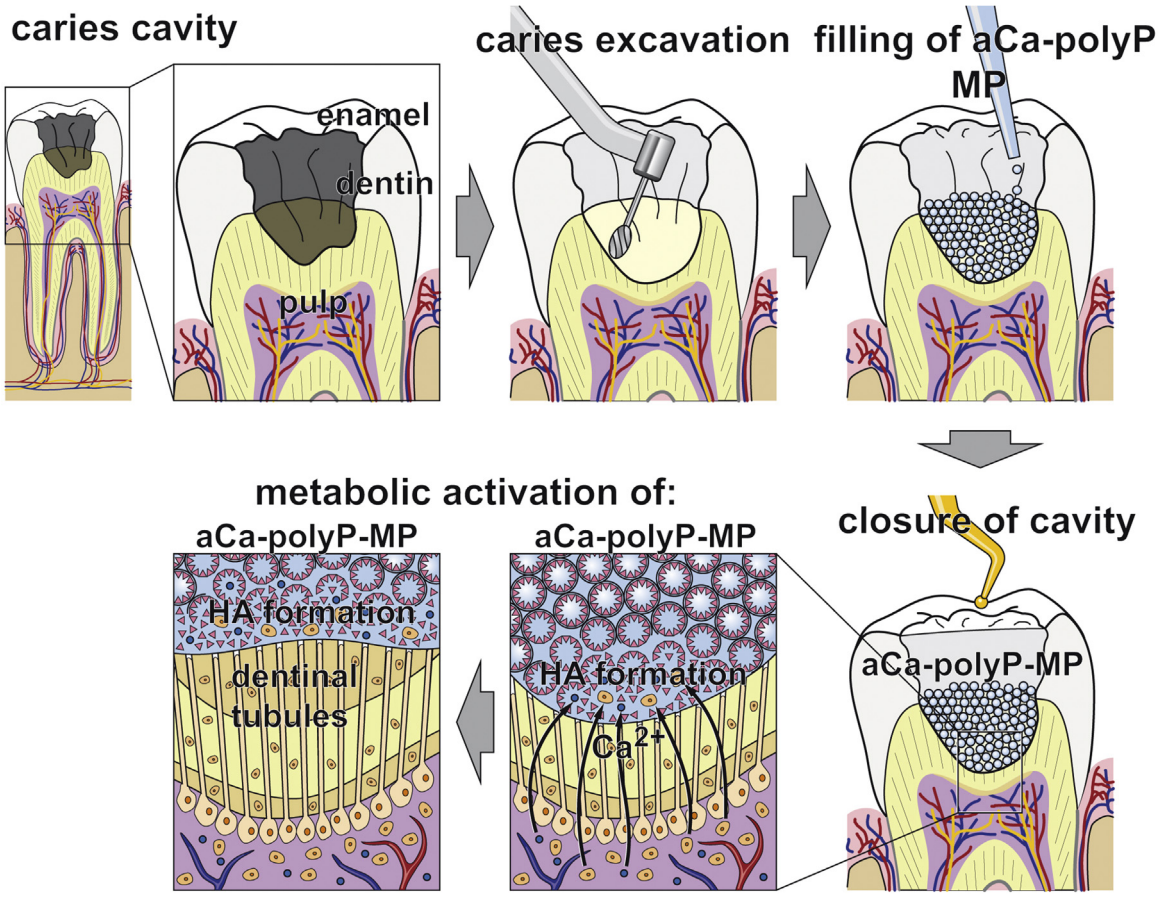

Fig. 8 – Application of polyP microparticles as material applicable for enamel reconstitution and dentin or dentinal tubules restoration (Scheme). The region(s) of caries decay and dentinal defects are overlayed by aCa-polyP-MP particles. Introduced into the biological environment the microparticles undergo coacervate formation a process during which polyP gains its beneficial ameliorating property.

cleavage to ortho-phosphate by the ALP. The polymer can also stabilize the precursor of bone-mineral ACC, which certainly promotes the synthesis of the Ca-polyP mineral [17]. In addition, amorphous polyP releases metabolic energy during and after hydrolytic cleavage by the ALP [26], an enzyme which is abundant in saliva [72]. The ALP is a processing enzyme [73] that, like in ATP, cleaves off one terminal hydrogen phosphate and one additional proton per anhydride linkage from polyP [74–76]. This finding implies that during polyP degradation a local pH shift occurs, which can lead to a localized demineralization of the HA and thus to an increase microroughness of the respective surface [77]. The concentration of Ca^{2+} in human saliva is ≈1 mM and the phosphate concentration is ≈ 3.5 mM [51]. However, the extent of mineralization in the saliva is also dependent on the protein content. Here polyP provides a distinguished feature. In an aqueous system without protein, the aCa-polyP-MP are not undergoing dissolution [78]. However, after exposure to protein, polyP undergoes rapid coacervation under concomitant release of the biological potency. In turn, polyP is activated in parallel with an increase in protein levels.

polyP as an “ancient” molecule found in all living organisms from bacteria to mammals (reviewed in Ref.: [22]) is known to be synthesized and metabolized by both caries-active and caries-inactive Streptococci bacteria living in the oral cavity [79–81]. In these studies, no direct causal relationship between the biological polyP turnover and the dental caries process has been addressed. Recently, it has been proposed that polyP-accumulating bacteria that are also present in the oral biofilm contribute to undersaturated phosphate conditions that can lead to mineral dissolution and caries progression [82]. While the correlations between polyP-producing bacteria and acid production and a relative phosphate deprivation could indeed occur locally, the beneficial/ameliorating effect of polyP on HA integrity was not the task of these papers. There is experimental evidence demonstrating that an increase in bacterial polyP metabolism is also associated with an increased sequestering of the polymer [83], which has a beneficial effect on the HA dissolution rate [84]. It has been found that the polymer reduces the baseline dissolution rate of HA, an effect that is even enhanced by fluoride.

It has been suggested that polyP is released by bacteria in the form of particles [85]. In the mammalian system, polyP is stored and released in the form of nanoparticles/microparticles (reviewed in Ref.: [22]) in every type of cells, and particularly in blood platelets (see Refs.: [25,86]).

It has recently been shown that these particles released on the surface of platelets are the causative components of the procoagulant activity of these cells [87].

It has been possible to fabricate, in a biomimetic way, the physiologically occurring polyP with a chain length of ≈40 phosphate units as amorphous aCa-polyP-MP [27]. These particles, when packed into a dentifrice [26,46,47], contribute to the resealing of teeth defects and are even toxic for the cariogenic bacterium *Streptococcus mutans* [47]. As shown in the present contribution the HA-promoting activity of polyP is seen in both the enamel and dentin regions of human teeth. Data are summarized demonstrating that toothpaste supplemented with 3% [w/w] of aCa-polyP-MP shows a prolonged retention time compared to the paste without polyP on the surface of the enamel. While the paste without polyP is almost completely removed after the 6 d treatment period, a substantial amount of deposits on the enamel brushed with polyP-containing dentifrice has been identified. By analysis of the remaining deposits with EDX, this material could be identified as Ca-polyP. Moreover, by applying the quantitative approach, it could be shown that the Ca/P atomic ratio increased from 0.6, found within the starting polyP-containing paste to 0.93 ± 0.18 after a treatment of the enamel for 3 d and finally to 1.50 ± 0.23, after the 6 d incubation period. The latter figures support the view that polyP present on the enamel accumulates Ca^{2+} with increasing duration of treatment. This supports the view that the microparticles tend to accumulate Ca^{2+} over phosphate to over-stoichiometric ratio values of >2 [29]. The Ca/P atomic ratio of 1.50 is close to that characteristic for geological HA, which is around 1.67 (reviewed in Ref.: [88,89]. The polyP-mediated sealing effect on tooth damages is observed both on the enamel (covering carious lesions) and on the dentin (closing of the dentinal tubules). As shown before, these polyP-mediated deposits are sustainable and resistant to ultrasonication [26].

In the focus of the present study is the observation that polyP, applied as aCa-polyP-MP, induces a regeneration mineralic zone on the surface of the enamel, as visualized by SRXTM. The polyP particles embedded in a glycerol solvent initiate this induced mineralization process. While the polyP-lacking glycerol samples do not have a promoting effect on mineralization process during incubation with artificial saliva, the polyP-glycerol-treated enamel samples are covered with a ≈20 μm thick "induced mineral deposit". This result supports the view that polyP accelerates the natural maturation phases of HA derived from ACP [90].

5. Conclusion

Not only organic but also inorganic macromolecules/deposits in the human body undergo metabolic changes that are driven by enzymes in addition to physical parameters. This also applies to physiological and pathological alterations of the mineralic teeth. In these structures, enzymes likewise substantially contribute to alterations, such as glucansucrase in dental plaque formation [91] or amylase-α and carbonic anhydrase-VI [92]. The concept of the present study is based on a biomimetic approach for ameliorating or even repairing hard tissue defects of the teeth. Evidence, also presented in this study, accumulates that polyP, particularly when produced in the form of microparticles, aCa-polyP-MP, induces the formation of a resealing layer on teeth decay regions. Since the material accelerates the restoration process not only on the enamel but also on the dentin, the polyP appears to be a promising dental filling material which elicits regenerative activity (Fig. 8).

As outlined in the present study, the amorphous particles, when packed in a dentifrice, form a mineralic layer on both mineral zones of the teeth. This process is further enhanced by the ions present in saliva, as shown here. In addition, the saliva contains proteins/mucoproteins in the range of 1 mg/ml [93]. In light of our recent study [78], these proteinaceous components of the saliva will surely reduce the zeta potential of the particles and promote the conversion of aCa-polyP-MP into the coacervate form, which is the biocompatible and ultimately bioactive form of the microparticles. During this process, polyP is enzymatically cleaved by the ALP, resulting in the release of the ortho-phosphate building unit for HA and of metabolic energy required for the energy-consuming anabolic metabolic processes that likely involve a second enzyme, the carbonic anhydrase IX, to synthesize the amorphous calcium carbonate bio-seeds which trigger calcium phosphate bone mineral deposition ([94]; reviewed in Ref.: [29]). Based on the available data, an inlay or onlay material containing aCa-polyP-MP, as outlined in Fig. 8, will shift to the bioactive form of polyP through the metabolic exchange processes mediated by the dentin tubules after filling into the decay region, and by integration processes of the polyP into the HA material.

In addition, if this approach proves successful, the use of amorphous polyP particles as fillers for caries lesions can be anticipated

Acknowledgements

W.E.G.M. is the holder of an ERC Advanced Investigator Grant (Grant No. 268476) and has received three ERC-PoC grants (Si-Bone, Grant No. 324564; MorphoVES-PoC, Grant No. 662486; and ArthroDUR Grant No. 767234). In addition, this work was supported by a grant from the Federal Ministry for Education and Research (NanoOsMed; Grant No. 01DH17034A), the BiomaTiCS research initiative of the University Medical Center Mainz and the International Human Frontier Science Program.

REFERENCES

[1] Sasaki K, Suzuki O, Takahashi N, editors. Interface oral health science 2016-innovative research on biosis—abiosis intelligent interface. Springer Nature Singapore Pvt. Ltd.; 2017.
[2] Melo MA, Guedes SF, Xu HH, Rodrigues LK. Nanotechnology-based restorative materials for dental caries management. Trends Biotechnol 2013;31:459–67.
[3] Wang XH, Schröder HC, Müller WEG. Enzymatically synthesized inorganic polymers as morphogenetically active bone scaffolds: application in regenerative medicine. Int Rev Cell Mol Biol 2014;313:27–77.
[4] Westbroek P, De Jong EW, editors. Biomineralization and biological metal accumulation. Biological and geological

perspectives. Dordrecht-Boston-London: D. Reidel Publishing Company; 1983.
[5] Lowenstam HA, Weiner S. On biomineralization. New York: Oxford University Press; 1989.
[6] Mann S. In: Mann S, Webb J, Williams RJP, editors. Biomineralization: chemical and biochemical perspectives. New York: VCH Publishers; 1988.
[7] Addadi L, Joester D, Nudelman F, Weiner S. Mollusk shell formation: a source of new concepts for understanding biomineralization processes. Chem Europ J 2006;12:981–7.
[8] Krasko A, Gamulin V, Seack J, Steffen R, Schröder HC, Müller WEG. Cathepsin, a major protease of the marine sponge *Geodia cydonium*: purification of the enzyme and molecular cloning of cDNA. Molec Mar Biol Biotechnol 1997;6:296–307.
[9] Shimizu K, Cha J, Stucky GD, Morse DE. Silicatein alpha: cathepsin L-like protein in sponge biosilica. Proc Natl Acad Sci U S A 1998;95:6234–8.
[10] Wang XH, Schröder HC, Wang K, Kaandorp JA, Müller WEG. Genetic, biological and structural hierarchies during sponge spicule formation: from soft sol-gels to solid 3D silica composite structures. Soft Matter 2012;8:9501–18.
[11] Müller WEG, Schröder HC, Burghard Z, Pisignano D, Wang XH. Silicateins — A novel paradigm in bioinorganic chemistry: enzymatic synthesis of inorganic polymeric silica. Chem Eur J 2013;19:5790–804.
[12] Armirotti A, Damonte G, Pozzolini M, Mussino F, Cerrano C, Salis A, et al. Primary structure and post-translational modifications of silicatein beta from the marine sponge *Petrosia ficiformis* (Poiret, 1789). J Proteome Res 2009;8:3995–4004.
[13] Schröder HC, Wang XH, Manfrin A, Yu SH, Grebenjuk VA, Korzhev M, et al. Silicatein: acquisition of structure-guiding and structure-forming properties during maturation from the pro-silicatein to the silicatein form. J Biol Chem 2012;287:22196–2205.
[14] Pellegrino ED, Blitz RM. Mineralization in the chick embryo. I. Monohydrogen phosphate and carbonate relationships during maturation of the bone crystal complex. Calcif Tissue Res 1972;10:128–35.
[15] Wang XH, Schröder HC, Müller WEG. Enzyme-based biosilica and biocalcite: biomaterials for the future in regenerative medicine. Trends Biotechnol 2014;32:441–7.
[16] Weiner S, Mahamid J, Politi Y, Ma Y, Addadi L. Overview of the amorphous precursor phase strategy in biomineralization. Front Mater Sci China 2009;3:104–8.
[17] Müller WEG, Neufurth M, Huang J, Wang K, Feng Q, Schröder HC, et al. Non-enzymatic transformation of amorphous $CaCO_3$ into calcium phosphate mineral after exposure to sodium phosphate *in vitro*: implications for in vivo hydroxyapatite bone formation. ChemBioChem 2015;16:1323–32.
[18] Eanes ED, Meyer JL. The maturation of crystalline calcium phosphates in aqueous suspensions at physiologic pH. Calcif Tissue Res 1977;23:259–69.
[19] Chung CH, Golub EE, Forbes E, Tokuoka T, Shapiro IM. Mechanism of action of beta-glycerophosphate on bone cell mineralization. Calcif Tissue Int 1992;51:305–11.
[20] Boskey AL, Guidon P, Doty SB, Stiner D, Leboy P, Binderman I. The mechanism of beta-glycerophosphate action in mineralizing chick limb-bud mesenchymal cell cultures. J Bone Miner Res 1996;11:1694–702.
[21] Leyhausen G, Lorenz B, Zhu H, Geurtsen W, Bohnensack R, Müller WEG, et al. Inorganic polyphosphate in human osteoblast-like cells. J Bone Miner Res 1998;13:803–12.
[22] Morrissey JH, Choi SH, Smith SA. Polyphosphate: an ancient molecule that links platelets, coagulation, and inflammation. Blood 2012;119:5972–9.
[23] Lorenz B, Schröder HC. Mammalian intestinal alkaline phosphatase acts as highly active exopolyphosphatase. Biochim Biophys Acta 2001;1547:254–61.
[24] Omelon S, Georgiou J, Variola F, Dean MN. Colocation and role of polyphosphates and alkaline phosphatase in apatite biomineralization of elasmobranch tesserae. Acta Biomater 2014;10:3899–910.
[25] Müller WEG, Tolba E, Feng Q, Schröder HC, Markl JS, Kokkinopoulou M, et al. Amorphous Ca^{2+} polyphosphate nanoparticles regulate the ATP level in bone-like SaOS-2 cells. J Cell Sci 2015;128:2202–7.
[26] Müller WEG, Wang S, Neufurth M, Kokkinopoulou M, Feng Q, Schröder HC, et al. Polyphosphate as a donor of high-energy phosphate for the synthesis of ADP and ATP. J Cell Sci 2017;130:2747–56.
[27] Müller WEG, Tolba E, Schröder HC, Wang S, Glaßer G, Muñoz-Espí R, et al. A new polyphosphate calcium material with morphogenetic activity. Mater Lett 2015;148:163–6.
[28] Lander N, Cordeiro C, Huang G, Docampo R. Polyphosphate and acidocalcisomes. Biochem Soc Trans 2016;44:1–6.
[29] Wang XH, Schröder HC, Müller WEG. Amorphous polyphosphate, a smart bioinspired nano-/bio-material for bone and cartilage regeneration: towards a new paradigm in tissue engineering. J Mat Chem B 2018;6:2385–412.
[30] Habraken W, Habibovic P, Epple M, Bohner M. Calcium phosphates in biomedical applications: materials for the future? Mater Today 2016;19:69–87.
[31] Habraken WJ, Tao J, Brylka LJ, Friedrich H, Bertinetti L, Schenk AS, et al. Ion-association complexes unite classical and non-classical theories for the biomimetic nucleation of calcium phosphate. Nat Commun 2013;4:1507.
[32] Weiner S, Traub W, Wagner HD. Lamellar bone: structure-function relations. J Struct Biol 1999;126:241–55.
[33] Nightingale JP, Lewis D. Pole figures of the orientation of apatite in bones. Nature 1971;232:334–5.
[34] Fratzl-Zelman N, Fratzl P, Hörandner H, Grabner B, Varga F, Ellinger A, et al. Matrix mineralization in MC3T3-E1 cell cultures initiated by beta-glycerophosphate pulse. Bone 1998;23:511–20.
[35] Omelon SJ, Grynpas MD. Relationships between polyphosphate chemistry, biochemistry and apatite biomineralization. Chem Rev 2008;108:4694–715.
[36] Thian ES, Konishi T, Kawanobe Y, Lim PN, Choong C, Ho B, et al. Zinc-substituted hydroxyapatite: a biomaterial with enhanced bioactivity and antibacterial properties. J Mater Sci Mater Med 2013;24:437–45.
[37] Thouverey C, Bechkoff G, Pikula S, Buchet R. Inorganic pyrophosphate as a regulator of hydroxyapatite or calcium pyrophosphate dihydrate mineral deposition by matrix vesicles. Osteoarthritis Cartilage 2009;17:64–72.
[38] Demer LL, Tintut Y. Pitting phosphate transport inhibitors against vascular calcification. Circ Res 2006;98:857–9.
[39] O'Neill WC. Pyrophosphate, alkaline phosphatase, and vascular calcification. Circ Res 2006;99:e2.
[40] Orimo H. The mechanism of mineralization and the role of alkaline phosphatase in health and disease. J Nippon Med Sch 2010;77:4–12.
[41] Omelon S, Georgiou J, Henneman ZJ, Wise LM, Sukhu B, Hunt T, et al. Control of vertebrate skeletal mineralization by polyphosphates. PLoS One 2009:e5634.
[42] Müller WEG, Tolba E, Schröder HC, Muñoz-Espí R, Diehl-Seifert B, Wang XH. Amorphous polyphosphate-hydroxyapatite: a morphogenetically active substrate for bone-related SaOS-2 cells *in vitro*. Acta Biomat 2016;31:358–67.
[43] Sfeir C, Ho L, Doll BA, Azari KMD, Hollinger J. Fracture repair. In: Lieberman JR, Friedlaender GE, editors. Bone

regeneration and repair: biology and clinical applications. Totowa, NJ: Humana Press Inc.; 2005. p. 21–44.
[44] Huang Y, Bornstein MM, Lambrichts I, Yu HY, Politis C, Jacobs R. Platelet-rich plasma for regeneration of neural feedback pathways around dental implants: a concise review and outlook on future possibilities. Int J Oral Sci 2017;9:1–9.
[45] Cornish CJ, Posen S. Human salivary alkaline phosphatase. Clin Chim Acta 1968;20:387–91.
[46] Müller WEG, Neufurth M, Tolba E, Wang S, Geurtsen W, Feng Q, et al. A biomimetic approach to ameliorate dental hypersensitivity by amorphous polyphosphate microparticles. Dent Mater 2016;32:775–83.
[47] Müller WEG, Neufurth M, Tolba E, Ackermann M, Korzhev M, Wang S, et al. Bifunctional dentifrice: amorphous polyphosphate a regeneratively active sealant with potent anti-Streptococcus mutans activity. Dent Mater 2017;33:753–64.
[48] Müller WEG, Ackermann M, Neufurth M, Tolba E, Wang S, Feng Q, et al. A novel biomimetic approach to repair enamel cracks/carious damages and to reseal dentinal tubules by amorphous polyphosphate. Polymers 2017;9:120.
[49] Stampanoni M, Groso A, Isenegger A, Mikuljan G, Chen Q, Bertrand A, et al. Trends in synchrotron-based tomographic imaging: the SLS experience. Developments in X-Ray Tomography. Proc. SPIE 2006, 6318 63180 M.
[50] Pabst AM, Wagner W, Kasaj A, Gebhardt S, Ackermann M, Astolfo A, et al. Synchrotron-based X-ray tomographic microscopy for visualization of three-dimensional collagen matrices. Clin Oral Investig 2015;19:561–4.
[51] Baumann T, Bereiter R, Lussi A, Carvalho TS. The effect of different salivary calcium concentrations on the erosion protection conferred by the salivary pellicle. Sci Rep 2017;7:12999.
[52] Kurihara H, Kataumi T, Tanase K, Eda K, Ikeda H, Ogihara T, et al. Mineral transfer between enamel and artificial saliva. Dent Oral Craniofac Res 2017;3:1–4.
[53] Ashkenazi D, Gitler H, Stern A, Tal O. Metallurgical investigation on fourth century BCE silver jewellery of two hoards from Samaria. Sci Rep 2017;7:40659.
[54] Petrie A, Watson P. Statistics for veterinary and animal science. Oxford, UK: Wiley-Blackwell; 2013. p. 85–99.
[55] Reyes-Gasga J, Martínez-Piñeiro EL, Brès EF. Crystallographic structure of human tooth enamel by electron microscopy and X-ray diffraction: hexagonal or monoclinic? J Microsc 2012;248:102–9.
[56] Deakins M, Burt RL. The deposition of calcium, phosphorus, and carbon dioxide in calcifying dental enamel. J Biol Chem 1944;156:77–83.
[57] Zaichick V, Zaichick S. The effect of age and gender on calcium, phosphorus, and calcium-phosphorus ratio in the crowns of permanent teeth. EC Dent Sci 2016;5(2):1030–46.
[58] Moyaho-Bernal de Los Angeles M, Contreras-Bulnes R, Rodríguez-Vilchis LE, Rubio-Rosas E, Scougall-Vilchis RJ, Centeno-Pedraza C. Morphological and chemical changes in human deciduous dentin after phosphoric acid, self-etching adhesive and Er: YAG laser conditioning. Microsc Res Tech 2018;81:494–501.
[59] Torres MG, Santos Ada S, Neves FS, Arriaga ML, Campos PS, Crusoé-Rebello I. Assessment of enamel-dentin caries lesions detection using bitewing PSP digital images. J Appl Oral Sci 2011;19:462–8.
[60] Schilke R, Lisson JA, Bauss O, Geurtsen W. Comparison of the number and diameter of dentinal tubules in human and bovine dentine by scanning electron microscopic investigation. Arch Oral Biol 2000;45:355–61.
[61] Sato Y, Sato T, Niwa M, Aoki H. Precipitation of octacalcium phosphates on artificial enamel in artificial saliva. J Mater Sci Mater Med 2006;17:1173–7.
[62] Nanci A, Ten Cate AR. Ten Cate's oral histology: development, structure, and function. 7th ed. London: Mosby; 2008.
[63] Arends J, Jongebloed WL. Crystallites dimensions of enamel. J Biol Buccale 1978;6:161–71.
[64] Goldberg M, Kulkarni AB, Young M, Boskey A. Dentin: structure, composition and mineralization. Front Biosci (Elite Ed) 2011;3:711–35.
[65] Cate JM, Arends J. Remineralization of artificial enamel lesions in vitro. Caries Res 1977;11:277–86.
[66] Grynpas MD, Bonar LC, Glimcher MJ. Failure to detect an amorphous calcium-phosphate solid phase in bone mineral: a radial distribution function study. Calcif Tissue Int 1984;36:291–301.
[67] Boskey AL. Mineralization of bones and teeth. Elements 2007;3:387–93.
[68] Carden A, Morris MD. Application of vibrational spectroscopy to the study of mineralized tissues (review). J Biomed Opt 2000;5:259–68.
[69] Verdelis K, Lukashova L, Wright JT, Mendelsohn R, Peterson MGE, Doty S, et al. Maturational changes in dentin mineral properties. Bone 2007;40:1399–407.
[70] Kianoush N, Adler CJ, Nguyen KA, Browne GV, Simonian M, Hunter N. Bacterial profile of dentine caries and the impact of pH on bacterial population diversity. PLoS One 2014;9:e92940.
[71] Dawes C. What is the critical pH and why does a tooth dissolve in acid? J Can Dent Assoc 2003:722–4.
[72] Jazaeri M, Malekzadeh H, Abdolsamadi H, Rezaei-Soufi L, Samami M. Relationship between salivary alkaline phosphatase enzyme activity and the concentrations of salivary calcium and phosphate ions. Cell J Spring 2015;17:159–62.
[73] Golub EE, Boesze-Battaglia K. The role of alkaline phosphatase in mineralization. Curr Opin Orthop 2007;18:444–8.
[74] Demenis MA, Leone FA. Kinetic characteristics of ATP hydrolysis by a detergent-solubilized alkaline phosphatase from rat osseous plate. UBMB Life 2000;49:113–9.
[75] Dorozhkin SV. Dissolution mechanism of calcium apatites in acids: a review of literature. World J Methodol 2012;2:1–17.
[76] Kalra DD, Kalra DR, Kini PV, Prabhu CRA. Nonfluoride remineralization: an evidence-based review of contemporary technologies. J Dental Allied Sci 2014;3:24–33.
[77] Budz JA, Nancollas GH. The mechanism of dissolution of hydroxyapatite and carbonated apatite in acidic solutions. J Crystal Growth 1988;91:490–6.
[78] Müller WEG, Wang S, Tolba E, Neufurth M, Ackermann M, Muñoz-Espí RI, et al. Transformation of amorphous polyphosphate nanoparticles into coacervate complexes: an approach for the encapsulation of mesenchymal stem cells. Small 2018;27:e1801170.
[79] Luoma H. Uptake of phosphate by caries-active and caries-inactive streptococci. Arch Oral Biol 1968;13:1331–42.
[80] Tanzer JM, Krichevsky MI. Polyphosphate formation by caries conducive Streptococcus SL-1. Biochim Biophys Acta 1970;215:368–76.
[81] Bowden GH, Nash R, Speirs RL. The localization and retention of ^{32}P and ^{45}Ca within surface deposits of Streptococcus sanguis and the influence of such deposits on the release of these isotopes from enamel. Caries Res 1973;7:185–200.
[82] Breiland AA, Flood BE, Nikrad J, Bakarich J, Husman M, Rhee T, et al. Polyphosphate-accumulating bacteria: potential contributors to mineral dissolution in the oral cavity. Appl Environ Microbiol 2018, http://dx.doi.org/10.1128/AEM.02440-17.

[83] Zhang F, Blasiak LC, Karolin JO, Powell RJ, Geddes CD, Hill RT. Phosphorus sequestration in the form of polyphosphate by microbial symbionts in marine sponges. Proc Natl Acad Sci U S A 2015;112:4381–6.
[84] do Amaral JG, Delbem ACB, Pessan JP, Manarelli MM, Barbour ME. Effects of polyphosphates and fluoride on hydroxyapatite dissolution: a pH-stat investigation. Arch Oral Biol 2016;63:40–6.
[85] Gächter R, Meyer JS, Mares A. Contribution of bacteria to release and fixation of phosphorus in lake sediments. Limnol Oceanogr 1988;33:1542–58.
[86] Schröder HC, Müller WEG, editors. Inorganic polyphosphates biochemistry, biology, biotechnology. Progress in molecular and subcellular. Heidelberg: Biology-Springer Press; 1999.
[87] Verhoef JJ, Barendrecht AD, Nickel KF, Dijkxhoorn K, Kenne E, Labberton L, et al. Polyphosphate nanoparticles on the platelet surface trigger contact system activation. Blood 2017;129:1707–17.
[88] Zipkin I. The inorganic composition of bones and teeth. In: Schraer H, editor. Biological calcification: cellular and molecular aspects. New York: Appleton Century Crofts; 1970. p. 69–103.
[89] Eliaz N, Metoki N. Calcium phosphate bioceramics: a review of their history, structure, properties, coating technologies and biomedical applications. Mater (Basel) 2017;10(4):334.
[90] Rabadjieva D, Gergulova R, Titorenkova R, Tepavitcharova S, Dyulgerova E, Balarew C, et al. Biomimetic transformations of amorphous calcium phosphate: kinetic and thermodynamic studies. J Mater Sci Mater Med 2010;21:2501–9.
[91] Vujicic-Zagar A, Pijning T, Kralj S, López CA, Eeuwema W, Dijkhuizen L, et al. Crystal structure of a 117 kDa glucansucrase fragment provides insight into evolution and product specificity of GH70 enzymes. Proc Natl Acad Sci U S A 2010;107:21406–11.
[92] Borghi GN, Rodrigues LP, Lopes LM, Parisotto TM, Steiner-Oliveira C, Nobre-Dos-Santos M. Relationship among (amylase and carbonic anhydrase VI in saliva, visible biofilm, and early childhood caries: a longitudinal study. Int J Paediatr Dent 2017;27:174–82.
[93] Mandel ID, Thompson Jr RH, Ellison SA. Studies on the mucoproteins of human parotid saliva. Arch Oral Biol 1965;10:499–507.
[94] Wang XH, Schröder HC, Schlossmacher U, Neufurth M, Feng Q, Diehl-Seifert B, et al. Modulation of the initial mineralization process of SaOS-2 cells by carbonic anhydrase activators and polyphosphate. Calcif Tissue Int 2014;94:495–509.